# Development of a New Beam Intensity Monitor Prototype

Julia Redinger

*Faculty of Engineering, University of Alberta, Canada*

Supervised by: Inaki Ortega

*SY-BI-XEI, CERN*

(Dated: August 22, 2025)

## Abstract

There are many kinds of beam monitors at CERN (European Organization for Nuclear Research) to monitor the properties of the many beamlines at this facility. One such monitor is the XSCI (eXperimental SCIntillator paddle counter) intensity monitor. These monitors operate in air, which can negatively impact beam integrity. To solve this, a new XSCI design that can operate in vacuum has been developed. This new design must fit into existing infrastructure, requiring changes to the monitor such as modified light guide lengths, vacuum compatibility, and a different motor configuration. This report will discuss the assembly of a prototype of this new monitor, including the design of optical gluing components and the evaluation of the performance of light guides. Furthermore, this new design was tested in the beamline, and the efficiency was analyzed in comparison with existing detectors. The efficiency was found to be greater than 99.5% for most intensities, which exceeds the 98% efficiency cutoff set by the users of the new monitor, the beam physicists at CERN. As a result, this new design can be recommended as a replacement for current XSCI monitors.

**Contents**

## I. Introduction

CERN (European Organization for Nuclear Research) hosts the LHC (Large Hadron Collider), the largest particle collider in the world, as well as the associated accelerator and injector complex. This facility accelerates particles in numerous different beamlines, which are used for all kinds of scientific research [1]. The properties of all of these beamlines need to be closely monitored to ensure stable particle beams for all of the experiments at CERN [2]. This is the responsibility of the Beam Instrumentation Group (BI).

One of the monitors developed by the BI group is the XSCI beam intensity monitor, used in the North Experimental Area at the CERN Prévessin site [3]. The North Area is a fixed target experimental area using beam extracted from the SPS (Super Proton Synchrotron) ring, which is one of the accelerator rings at CERN [4]. The XSCI (eXperimental SCIntillator paddle counter) is a scintillator-based monitor that currently operates in air - the beam therefore has to cross two vacuum-air windows and a section of air for each monitor. To preserve beam integrity, a new design was developed by Mark Kirschbaum [5] to operate the assembly under vacuum as well as motorize the system to remove the monitor from the beamline when not in use. This new monitor must also be integrated into the existing vacuum tanks in the beamlines, and be able to share this tank with an existing monitor (the XBPF or eXperimental Beam Profile Fiber monitor, described below). This work describes the assembly, installation, and evaluation of this new design to ensure its feasibility.

## II. Existing Monitor

The existing XSCI monitor uses a plastic scintillator paddle placed in the beamline. Through the scintillation process [6], photons are generated by the charged particles in the beam, and pass through a series of light guides. These capture the photons and keep them in the system with the principle of total internal reflection. The scintillator is coupled to a PMT (photomultiplier tube) which collects the photons. The data collected can then be analyzed and intensity calculations can be performed [3]. See Figure 1 for an image of the current XSCI monitors.

Additionally, the current XSCI design is motorized. The paddle can be retracted from the beamline using an electric when not in use, so as to not interfere with the beam unnecessarily.

FIG. 1: Current XSCI monitor used for measuring beam intensity [3]

XSCI monitors currently operate in air. The beam therefore must cross two windows between vacuum and air, as well as a section of air, for each monitor. To avoid this, and preserve beam integrity, a new design with the XSCI in vacuum was proposed.

## III. New Monitor Design

The goal of the new intensity monitor design is to operate the XSCI under vacuum, to preserve the beam integrity as much as possible. This design must also include in/out motorization to remove the scintillator from the beam, and must also be compatible with the FISC (see below) tanks currently in the beamline. It must also be able to share the vacuum tank with existing XBPF (eXperimental Beam Profile Fiber monitor) detectors.

The FISC tanks are existing infrastructure used for the FISC detectors. FISC (Filament Scintillator Scanners) detectors operate by scanning a thin scintillating 'film' through the beam, which produces photons. These are readout using two PMTs, and are used to calculate the position and profile of the beam [7]. Since these detectors operate under vacuum, it is

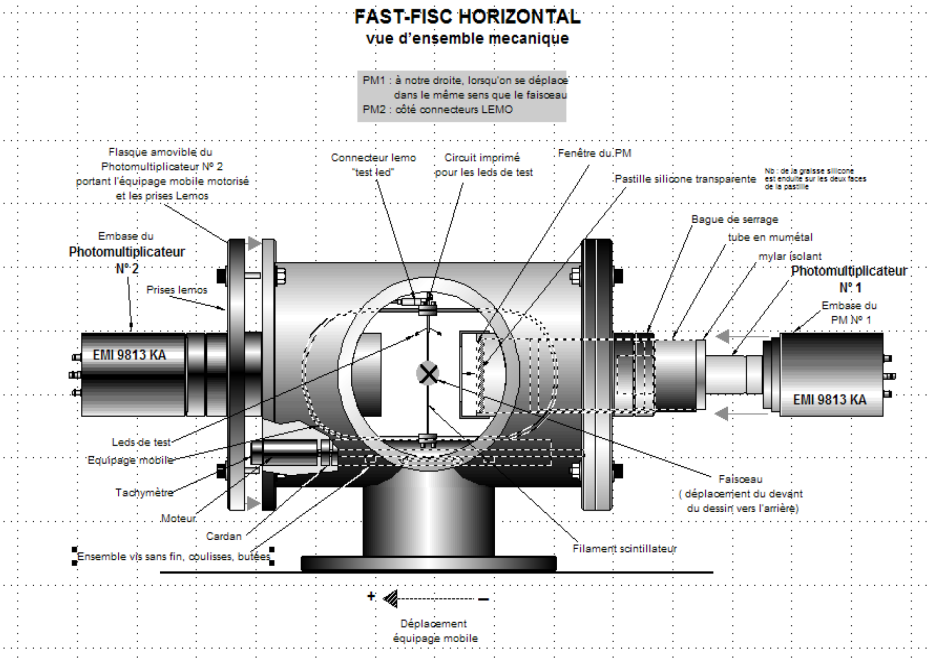


FIG. 2: A diagram of the FISC detector in the FISC tank [7]. The beam comes through the center (out of the page). One of the large flanges on the side was used for the installation of the new XSCI prototype.

convenient and more cost effective to use these tanks for the new intensity monitor. A diagram of the FISC tank is shown below in Figure 2.

The key requirements for this design include a high efficiency - the original design goal was for the efficiency to be greater than 98% [5]. This requirement was put forward by the beam physicists at CERN, who are the end users of this new monitor design.

The initial design was done by Mark Kirschbaum[1]. It features a scintillator disk like that of the previous XSCI monitors, flat light guides around the scintillator disk, and a specially-designed 'fishtail' light guide. While the scintillator can be under vacuum, it was not feasible to have the PMT be under vacuum - this would have come with several challenges, such as heating the circuits used in the PMT and the lack of space in the FISC tank that isn't in the path of the beam [5]. Therefore, a window design was created, where the light from the light guide is passed through an optical window, which is the boundary between the vacuum in the tank and the air outside, and to the PMT. This design can be seen in Figure 3, where

[1] Mark also designed another prototype with wavelength shifting fibers, which offered many advantages, including being more compact and more compatible with the FISC tanks. However, the wavelength shifting fibers have a poorer timing resolution. Given the importance of the resolution for measurements like the time of flight, the scintillator paddle design was ultimately chosen [5].

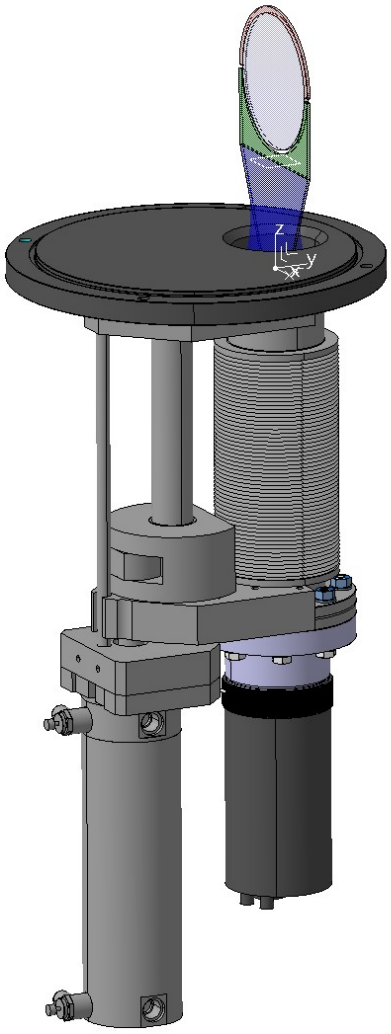


FIG. 3: The CAD design for the new XSCI. The scintillator disk, flat light guides, and the top of the fishtail light guide (in blue) are visible. The PMT is in the bellows, and the PMT base is in black.

the scintillator disk and the light guide (in blue) can be seen, and the optical window is located inside the bellows, above the PMT base[2]. The PMT itself is located in the bellows. See Figure 9b in Section IV B to see the optical window.

Also in the photo is a large circular flange (dark gray). This is how this assembly will interface with the FISC tank - it will be replace one of the flanges on the side of the FISC tank seen in Figure 2.

The motorization of this new design is possible with a pneumatic motor controlled by a

[2] Thank you to Benjamin Moser for this design and the image.

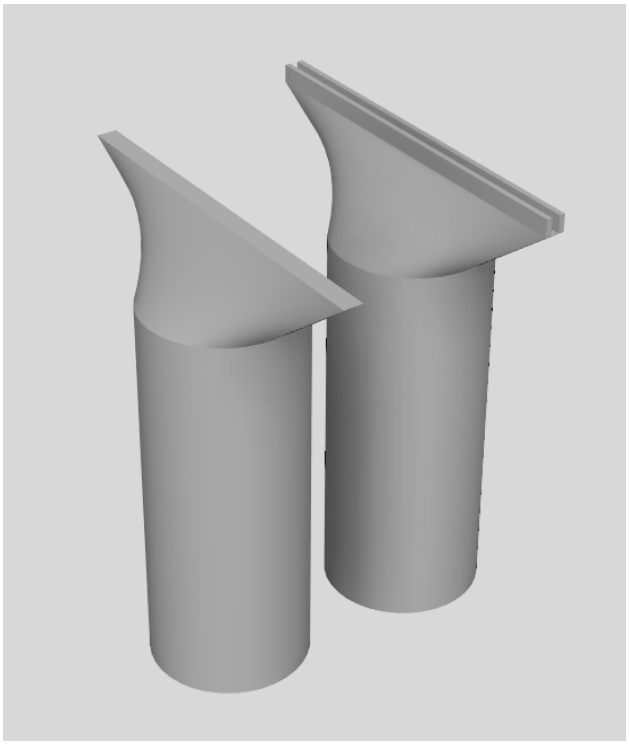

FIG. 4: The 3D model of the smooth and grooved fishtail light guides.

compressed air supply, which moves the bottom part of the assembly up, and pushes the scintillator up (into the path of the beam). This is different from the electric motor used by the existing monitors due to the vacuum force in the tank.

### A. Light Guides

There are three light guides in this design - two flat 'holder' light guides that surround the scintillator disk, and a fishtail light guide to couple to the PMT. The fishtail shape of the light guide is designed to transmit as many photons as possible from the thin, flat form factor of the edge of the flat light guides, to the circular shape of the PMT. It acts as an adapter between these two shapes.

Another design choice was the option of adding a slot/groove to the fishtail light guide, so that the flat light guide could be slid into the groove. The decision regarding the addition of a groove or not was investigated in this report and will be discussed further below. See Figure 4 for photos of the two.

Additionally, another change that was made in the new design is the length of the light

guide - to be able to fit the entire assembly in to the FISC tank, the fishtail light guide had to be shorter than usual. This was simulated by Mark [5], but this project was the first time that this new light guide design was tested.

## IV. Assembly

The components for the whole XSCI assembly were selected and ordered prior to the beginning of this project. The main focus of this report is to assemble the pieces and test them to evaluate the performance of the design.

### A. Optical Components

The optical components in this design (i.e. the scintillator disk, two flat light guides, and the fishtail light guide) all needed to be glued together. The glue used was Eljon EJ-500 optical cement, since optimal light transmission is needed between the components. This is a two part glue that requires 24 hours to set - therefore, the individual pieces need to be held together in a stable configuration for that amount of time while the glue sets.

To accomplish this, first the three flat pieces (the scintillator and the two flat light guides) were glued together. Since they are so thin, it was determined that the best way to do this was to glue them together while laying flat. To prevent the glue from leaking through the seams while drying, and therefore sticking the whole assembly to the gluing surface, a channel design was created in Autodesk Fusion and 3D printed. The Autodesk Fusion model can be seen in Figure 5a.

This design has a channel running underneath the seams (where the glue is) in the flat optical assembly. Therefore, each individual piece is supported (the scintillator is held up by the 'island' in the middle) but there is nothing under the seams with the glue. This allows the glue to 'bead' under the seams rather than sticking to anything. Figure 5b shows the optical pieces in the 3D printed design, with the seams where the glue is highlighted in yellow. The channel can be seen under the seams.

The design also has corner supports to align the bottom flat light guide, as well as removable tabs to hold the top (rounded) flat light guide. These tabs can be inserted after all three components have been glued together to hold them in place. Combined with pieces

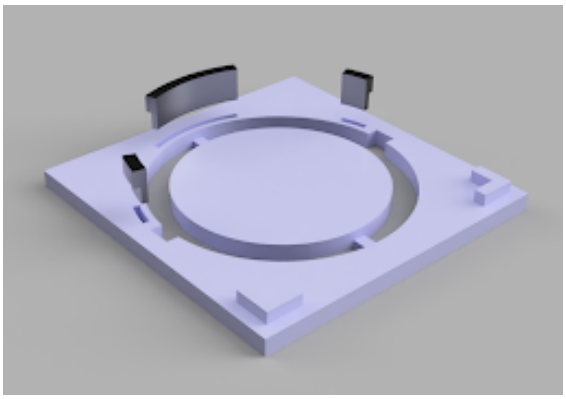

(a) Assembly designed and 3D printed to facilitate the gluing of the flat optical components (the scintillator disk and flat light guides).

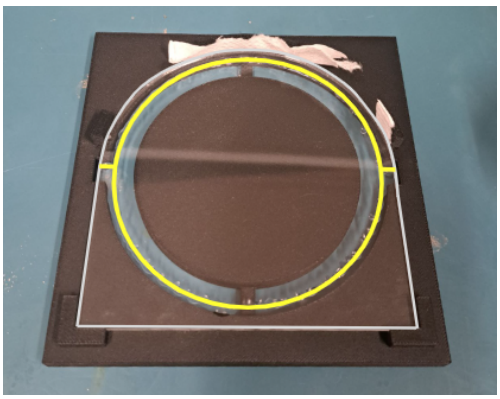

(b) An example of the gluing process. Seams with glue are marked in yellow, and have a channel underneath them to prevent the glue sticking to anything.

FIG. 5: The 3D printed assembly to facilitate the gluing of the flat optical components (the scintillator disk and flat light guides).

of paper towel to add extra thickness, they provide a bit of pressure to hold the piece together, and prevent air bubbles from forming in the glue (which will decrease the optical efficiency). Once again, see Figure 5b, where the tabs have been inserted with some paper towel to ensure adequate pressure.

The process used to glue the pieces together is as follows:

1. The glue is mixed first in a 4:1 (by weight) ratio of resin to hardener, according to the instructions.

2. A thin glass capillary was used to put small amounts of glue along the side of the bottom light guide (the one with the rectangular sides). Care was taken to ensure all spots were covered in a thin layer, with no missing spots. This piece was then placed in the 3D printed assembly, in the corner supports.

3. The scintillator disk was slid into the assembly and stuck to the bottom light guide.

4. Glue was applied to the top light guide in a similar manner to the bottom light guide. It was then slid onto the scintillator disk in the 3D printed support. Note that the tabs were removed for this part to make this easier.

5. The tabs can then be inserted, using pieces of thin material (such as paper towel) to ensure that the tabs were exerting enough pressure on the components to squeeze out any air bubbles. At this point, the assembly can be inspected for potential air bubbles or excess glue, and left to dry for 24 hours.

After this component has dried together, it can be removed from the 3D printed assembly. Next, it has to be glued to the fishtail light guide. This process depends on the design chosen: smooth or grooved.

*1. Smooth light guide gluing*

To glue the top assembly (scintillator disk + flat light guides) to the smooth light guide, a clamp assembly was put together to hold the top assembly in place on the smooth light guide. This was done with two clamps (to achieve the required angle), with foam taped to the inside of the clamp to prevent scratches on the top assembly. A base was also 3D printed and lined with foam to hold the fishtail light guide in place and also prevent it from getting scratched. Note that a 'notch' was taken out of this base to get it close enough to the clamp stand.

Once again, the glue was mixed and a thin glass capillary was used to put a line of glue on the fishtail light guide (which was in the 3D printed base). The top assembly was clamped at the correct angle, and then lowered onto the light guide. This final configuration can be seen in Figure 6.

*2. Grooved light guide gluing*

The grooved light guide gluing is much easier in principle, since all that is required is lining the groove with glue, and putting the top assembly in the groove. The groove should be the right size to hold the top assembly in place with no extra support required. The only thing to note is that care needs to be taken to prevent air bubbles from being trapped - the easiest way to do this is to insert one side in first (so that the whole top assembly is at an angle) and then slowly press the other side in, so all air bubbles get pushed out to the side.

In practice, however, the grooved light guide proved to be more difficult. Unfortunately, there were some tolerancing issues from the manufacturer. This required the groove to be

FIG. 6: The configuration to glue the top optical assembly to the smooth light guide.

modified, which resulted in the surface being less clear than it should be, as well as the fit still being tighter than it should have been.

The tight fit was not a major issue - it just meant that inserting the top assembly required a lot of force. Extra care was required to not snap the top assembly while still ensuring that no air bubbles got trapped. this required multiple attempts.

Additionally, sanding and polishing of the groove was required to try and get is as smooth and clear as possible. Sanding was done first with 600 grit sandpaper, followed by 800, 1000, and 1200. The sandpaper was folded to fit the groove and then slid back and forth through the groove for roughly 30 seconds. Next, Neoplex polishing paste was applied with a cloth and gently rubbed over the groove, and then rinsed off.

After two rounds of this, the groove was more clear. However, it was difficult to get rid of the scratches entirely, since sanding could only be done in the direction of the groove, and not in a more circular pattern. The translucent groove can be seen in Figure 7.

### B. Entire Assembly

After the optical components were glued together, the entire assembly could be put together. First, the ring clamp could be put on the base of the light guide. The ring clamp

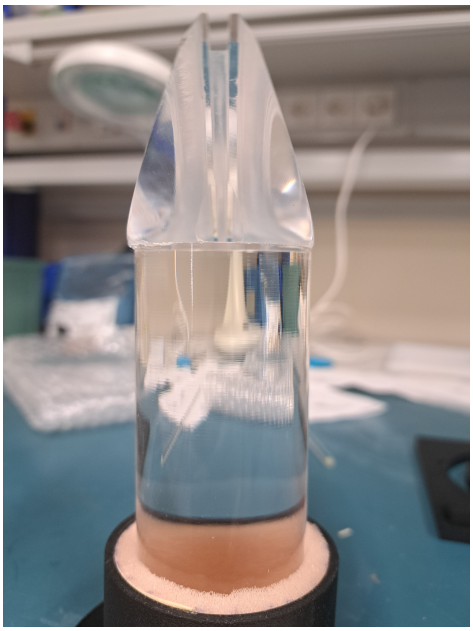

FIG. 7: The grooved fishtail light guide, with the translucent groove. Prior to sanding and polishing, the groove looked less transparent.

FIG. 8: The ring clamp on the bottom of the fishtail light guide.

can be seen in Figure 8. This clamp must be placed at the correct height and orientation so that the scintillator is perpendicular to the beam, and the nuts can be screwed onto the clamp properly. There are 3 small set screws that can be tightened to hold this clamp in place.

Next, the PMT and base need to be connected to the optical window assembly. These

components can be seen in Figure 9a, where the components from left to right are the PMT base, the screw ring to connect the PMT to the window assembly, the window assembly (with the light guide and scintillator assembly attached), and the PMT. The window assembly (which can be seen in Figure 9b) houses the PMT and the optical window that acts as the vacuum-air interface.

The PMT can simply be inserted into the PMT base. A coat of optical grease was then applied to the photocathode of the PMT (see Figure 9c), to help couple it to the optical window. The screw ring can be screwed onto the PMT base as well. Finally, the optical window assembly can be partially screwed into the screw ring on the PMT base. It is screwed in until the groove in the optical window assembly lines up with the holes in the screw ring - the clear plastic ring can then be inserted into the groove through the hole, which will hold the whole assembly together. See Figure 9d.

The scintillator and light guide assembly were also covered in a layer of tin foil. This may not be necessary, as the photons should remain inside the assembly due to total internal reflection, but was done to catch any stray photons and reflect them back into the light guides.

Now, the PMT/optical window assembly can be bolted onto the bellows. Next, the motor assembly needs to be hooked up to a compressed air line so that it can be pushed up (contracting the bellows) and the PMT part can be fully extended. This allows the scintillator assembly to be connected to the PMT assembly through the hole in the flange. This two-step process is necessary since the scintillator assembly cannot fit through the hole in the flange.

(This was done to minimize the size of the optical window. The larger the window, the more area needs to be pushed in/out of the assembly, and the larger the pressure. A smaller area means less force required to move everything.)

After coating the bottom of the light guide in another even coat of optical grease, it can be put on the optical window and the nuts can be put on. Finally, the assembly can be put on the large circular flange. The completed assembly can be seen in Figure 10.

Note that due to manufacturing errors, some parts of the assembly could not be fully put together. This includes a clip to hold the optical window in place, which could not be put in because the light guide diameter was too large. The bolts holding the end of the bellows onto the large flange could not all be put in, either, due to hole misalignment. See Section

(a) From left to right: the PMT base, the screw ring to connect the PMT to the window assembly, the window assembly (with the light guide attached), and the PMT.

(b) The optical window assembly. On top are the four bolts that hold the light guide in the ring clamp onto the optical window. The window is visible on top.

(c) The PMT photocathode with a layer of optical grease.

(d) The PMT base attached to the window assembly, with part of the clear ring used to connect them sticking out for demonstration.

FIG. 9: The parts and assembly process of the new XSCI.

FIG. 10: The completed assembly, including the PMT and its base, the scintillator and light guides, and the motor and bellows.

VIII A for more details.

## V. Testing

### A. Lab tests

Before the full assembly was put together, the scintillator/light guide/PMT assembly was tested in the lab. This was done both to verify functionality and to determine if the smooth or grooved light guide should be selected to be tested in the beam.

Another set of scintillator paddles were used to conduct a coincidence test with the new scintillator under test. The three scintillators were placed in a black box, such that the test scintillators were on top of an underneath the new scintillator. They were placed to minimize the chances of any particle going through both test scintillators, but not through the new scintillator. See Figure 11 for the test setup.

The test scintillators were powered by a battery supply, using potentiometers to control the voltage. Each test scintillator received 1 kV. The new scintillator was powered by an ISEG high voltage power supply.

The outputs of all 3 scintillators passed through a discriminator unit (with a threshold

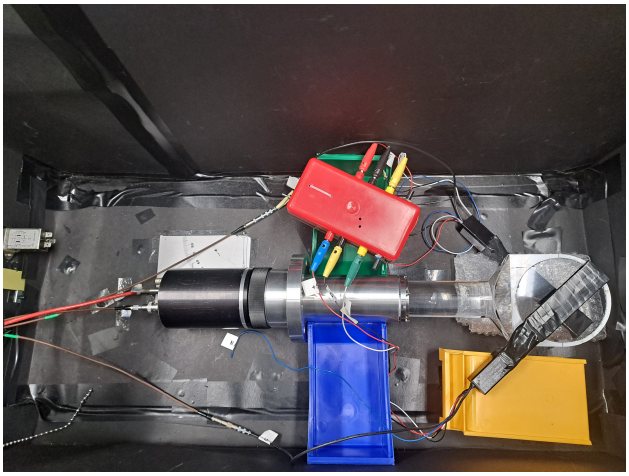

FIG. 11: The test setup for the new scintillators in a black box using two test scintillators.

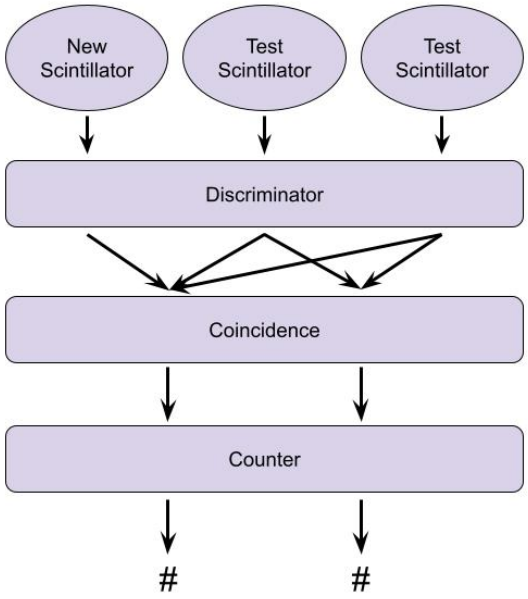


FIG. 12: The electronics used to test the new scintillator, using coincidences with two test scintillators.

of -30 mV) and then a coincidence unit. These were in a custom built NIM crate. Finally, a counter was used to measure hits. The logic for the electronics is shown in the diagram in Figure 12 - the number of hits from both test scintillators is compared to the number of hits in all three. The coincidence is used to reduce dark counts and other sources of noise.

Before testing all three scintillators together, a voltage scan was performed to determine the optimal operating voltage. The output count rates were recorded with different operating

voltages, using a radioactive source to generate large count rates. An additional scan without the source was also done to look at the dark rates. From this second scan, it was determined that above 1.91 kV, the dark count rate grew rapidly, so 1.91 kV was selected as the operating voltage.

Using this operating voltage, runs were conducted with cosmics for both the smooth and grooved light guides using the setup shown in Figure 11. Runs were limited in length by the battery powering the test scintillators.

For the smooth scintillator, the final counts before the battery died were 981 for the coincidence of all three scintillators, and 1064 for just the two test scintillators in coincidence. This gives an efficiency of 92.2%. For the grooved light guide, the counts were 2315 (the triple coincidence) out of 2422 (test scintillator coincidence), which is an efficiency of 95.6%. Therefore, the grooved scintillator was chosen to be put in the beamline for the full test.

### B. Beam Tests

The new XSCI assembly was tested in the beam, using an existing FISC tank at XFFH.041.437. This is on beamline H6 at the North Experimental Area at Prévessin. The flange was bolted onto the FISC tank, and the high voltage and signal cables were provided by existing infrastructure. Compressed air was used to extend the scintillator fully into the beam, where it was left for the duration of the tests.

An attempt was made to put the FISC tank under vacuum. This was unsuccessful, which was assumed to be due to the hols misalignment in the flange at the time. It was later discovered, after a lack of signal from the PMT, that the clamping force holding the light guide onto the rest of the assembly was not enough without the clip holding the optical window in place. Without this clip (which as mentioned earlier was not included due to a manufacturing error with the light guide tolerancing), the optical window and light guide/scintillator assembly were pushed into the FISC tank, which presumably resulted in the inability to put the system under vacuum as well as a lack of signal. A view of the optical window and light guide is in Figure 13.

The optical window and light guide were reinstalled, and all tests were done in air. The initial cause of the lack of PMT signal was also believed to be light leaks from the misaligned holes without bolts, so during the reinstallation, a new PMT was used, and black tape was

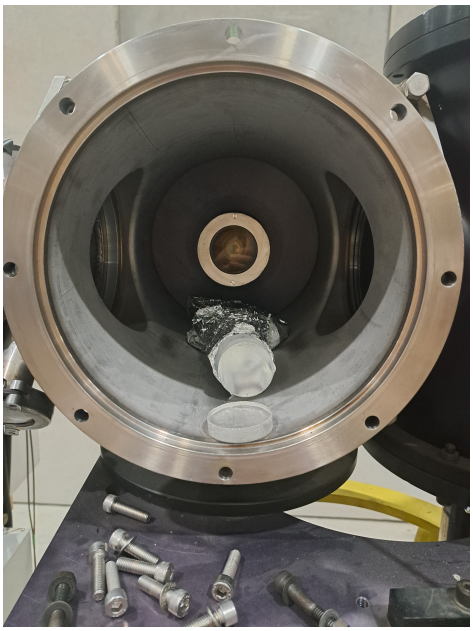

FIG. 13: The light guide/scintillator assembly and optical window after the vacuum test.

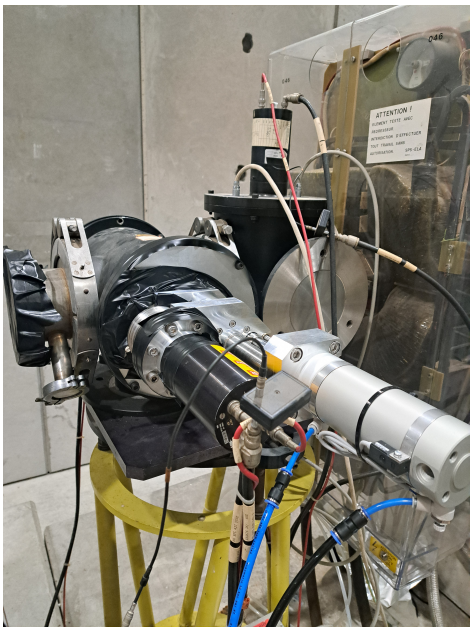

FIG. 14: The full XSCI prototype in the H6 beamline.

put over all seams and holes to prevent other light leaks. This should not be an issue in the final design, since if the system can be put under vacuum, no light should be able to get in. The full setup can be seen in Figure 14.

With the new PMT, another voltage scan was performed to determine the new optimal voltage to operate at. The PMT voltage was modified, and the output counts measured on

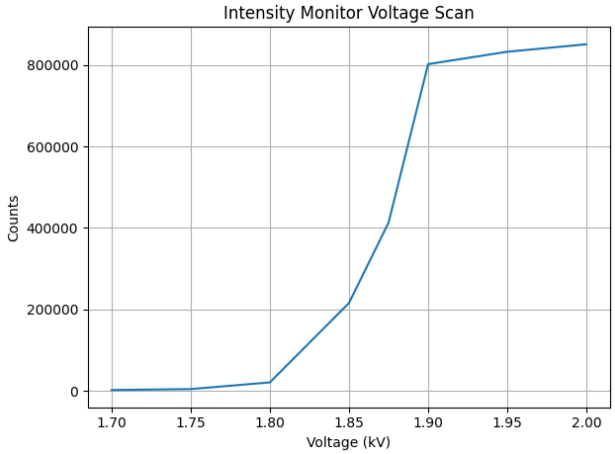


FIG. 15: Voltage scan performed for the PMT during the beam test around 16:30 on August 4, 2025.

Timber (XFFH.041.437:COUNTS_PM2) were recorded. The results are in Figure 15, where a notable plateau can be seen above 1.90 V. Since it is best to operate the PMT in a more stable region, the lower part (so as not to be too close to the maximum PMT voltage) of the plateau was selected, and the PMT was operated with a voltage of 1.91 kV.

With the monitor installed and the voltage applied, the data taking can begin.

## VI. Results

To get meaningful results, the output of the new monitor was compared to two other monitors downstream: XBH6.XSCI.041.438 and XBH6.XSCI.041.450. The coincidence of these two monitors was taken as the 'true' value, and it was compared to the coincidence of all three monitors, to reduce the effect of dark counts. Data was taken over a period of two days, but sections where the beam intensity was ramped up was used, to get an idea of the efficiency of the new detector over a range of intensities. One of these ramp-ups in particular will be studied here as a representative, since they all yielded very similar results.

First, the coincidence from reference detectors XBH6.XSCI.041.438 and 450 were compared to the coincidence counts of these two reference detectors and the new one. In Figure 16 below is the plot of the two counts.

For a range of intensities, the response of the new detector closely matches that of the existing ones. The efficiency of the new monitor (i.e. the ratio between the two coincidence

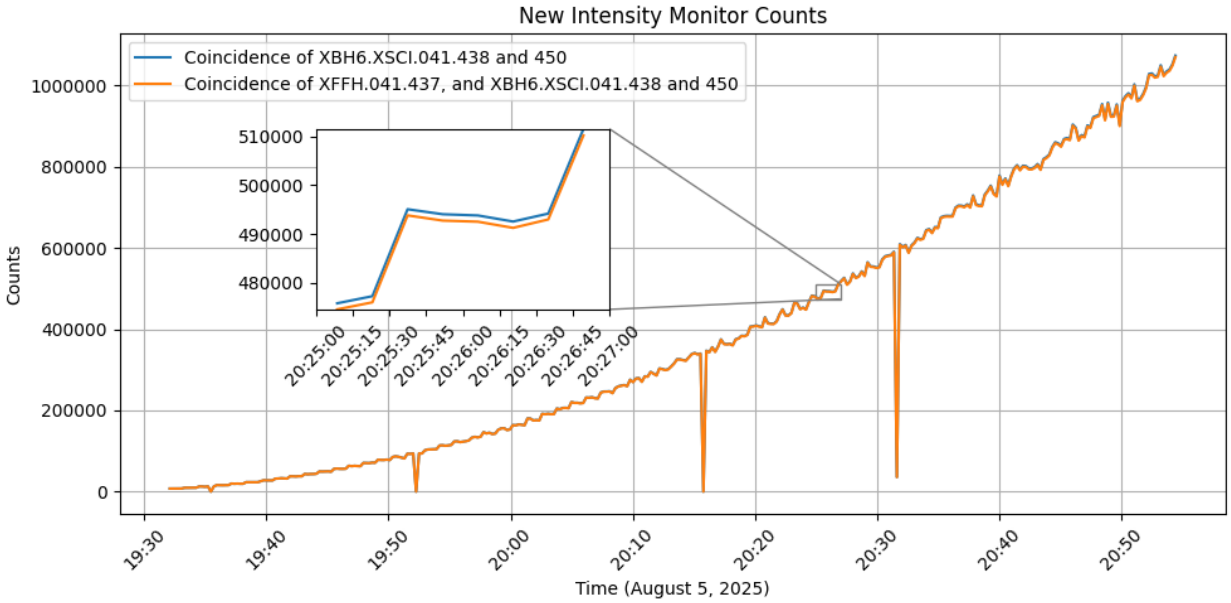


FIG. 16: The number of counts of two reference monitors in coincidence (XBH6.XSCI.041.438 and 450) compared to the coincidence of the two reference monitors and the new intensity monitor (XFFH.041.437).

counts) is above 99.5% for most intensities.

The efficiency as the beam was ramped in intensity is plotted against the number of counts (which is proportional to the intensity) in Figure 17 below. The efficiency is also plotted against the two collimator jaw widths, which is what was used to modify the beam intensity, in Figure 18.

There are two distinct features in these plots: first is the efficiency drop-off at low intensities, and the second is the slow falling off of the efficiency at high intensities. Further tests should be conducted with a more proper electronics setup before making any conclusions about the causes of these features. However, there are a few likely causes that will briefly be discussed here.

For the low intensity drop-off, this is likely caused by the stronger effect of dark counts at a lower intensity. Since the dark rate should not depend on intensity, its effect gets larger as the actual number of counts shrinks. This could result in a decrease in the efficiency.

For the high intensity slope, it is difficult to say what is causing this until further studies can be done. One possibility that was explored is the effect from overlapping counts - if two counts were sufficiently close together, they would be registered as one count. To estimate

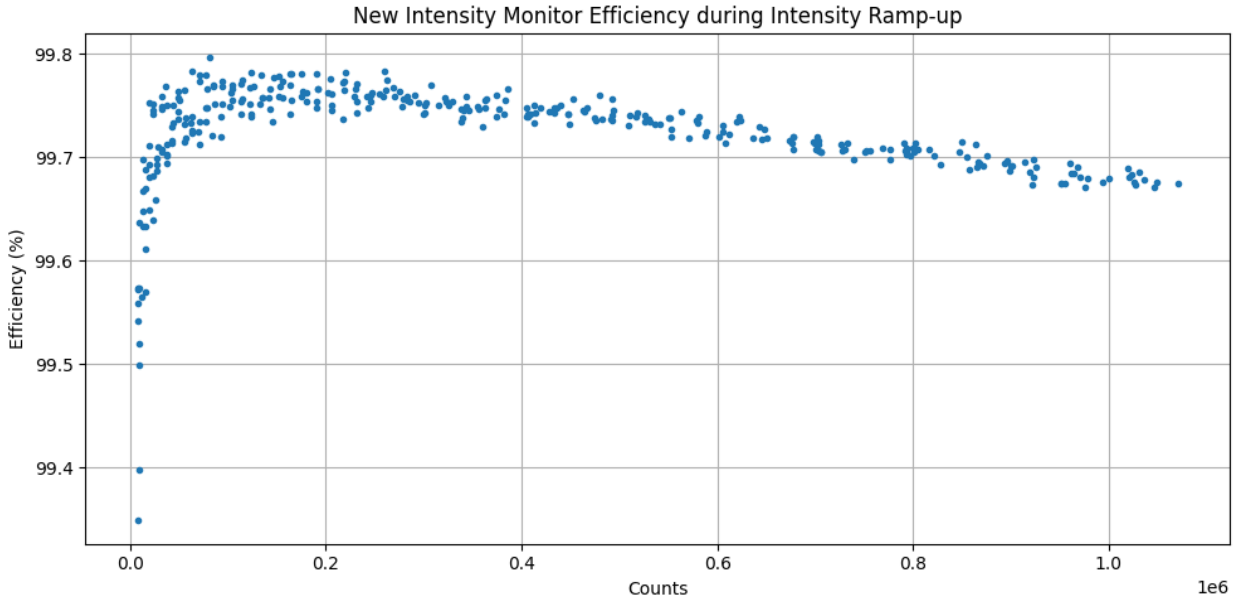


FIG. 17: The efficiency of the new intensity monitor as compared to the coincidence of two reference monitors.

how often this occurs, Poisson statistics were used.

From Poisson statistics, the probability of observing no counts in a time period t [8] (i.e. 'surviving' past time t) is

$$P(0|\lambda) = e^{-\lambda t}$$

where $\lambda$ is the count rate. To normalize it with respect to $t$:

$$\int_0^\infty A * P(0|\lambda)dt = 1 \rightarrow A * \int_0^\infty e^{-\lambda t}dt = 1 \rightarrow \frac{A}{\lambda} = 1 \rightarrow A = \lambda$$

Therefore, multiplying by $\lambda$, we can find the probability that $t$ is less than some $t_0$:

$$P(t \leq t_0) = \int_0^{t_0} \lambda e^{-\lambda t}dt = 1 - e^{-\lambda t_0}$$

For the the average maximum rate (231015.79 counts/s) and with the discriminator signal width of 30 ns ($t_0$ = 30 ns) this gives a maximal probability of 0.00691 or 0.691 % that multiple actual counts are being measured as one count. This probability is smaller for lower intensities.

These probabilities can be added to the efficiencies calculated earlier, to represent a maximum possible efficiency without the missed counts. This can be seen in Figure 19. The

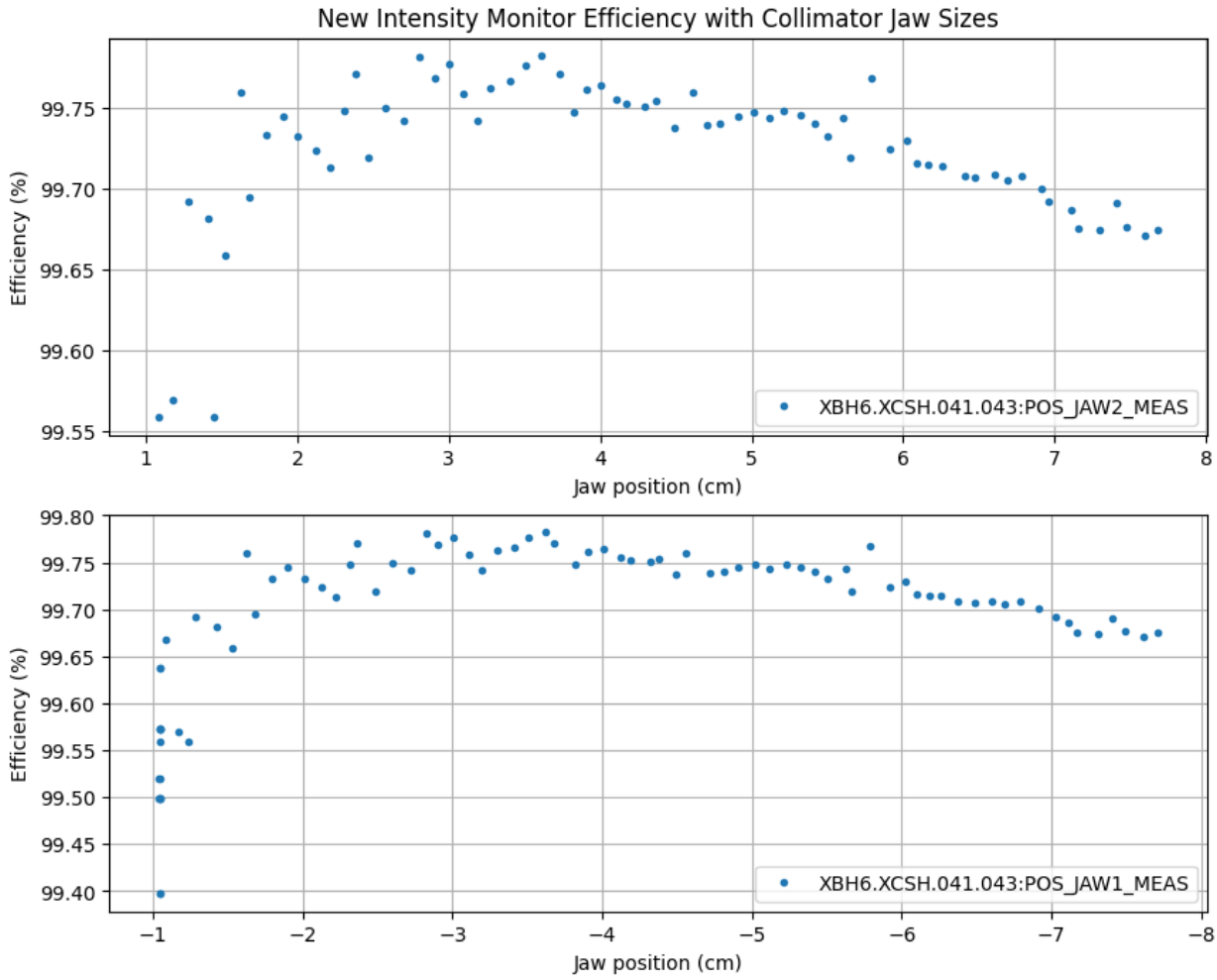


FIG. 18: The efficiency of the new intensity monitor plotted against the width of the two collimator jaws controlling the intensity.

corrected curve, however, has not fixed the slow drop-off at high intensities, and is unphysical (efficiencies greater than 100%). We can therefore conclude that while missing counts may still play a role in the shape of the efficiency curve, they are not the sole contributor. This is not entirely surprising, given that it is likely that if two counts are overlapping in one detector, they will overlap in the reference detectors as well. This means that the efficiency wouldn't be as affected. In conclusion, more studies will need to be done to determine the cause of this shape.


FIG. 19: The measured efficiencies as well as the efficiencies corrected for missing counts using Poisson statistics.

### A. Spurious Count Verification

Finally, calculations were performed to double check the rate of dark counts and spurious coincidences. First, the dark rate of each monitor was estimated, using a portion of the data where the beam was not on. The number of counts in that period for each detector was averaged to give a dark count number, and the dark rate was calculated using the 4.8 seconds for each spill.

The rate of false coincidences with the dark count of all three detectors (i.e. the rate at which a coincidence occurs as a result of a dark count in all three detectors simultaneously) can be estimated using the individual dark rates and the width of the discriminator pulses. This is calculated using the equation below [9], where DR is dark rate and w is the width of the discriminator pulse:

$$\text{rate} = 3 \times w^2 \times \text{DR}_{\text{new}} \times \text{DR}_{\text{ref 1}} \times \text{DR}_{\text{ref 2}} \tag{1}$$

Using a signal width of 30 ns this yields a false coincidence rate of 2.355e-11 counts/s. This is a sufficiently low number and can reasonably be ignored.

Additionally, we can look at the expected rate at which there is a coincidence between

the dark counts of the new monitor and actual hits (i.e. the coincidence of the two reference detectors). Since the actual rate is dependent on intensity, the highest intensity rate was considered, as rates at lower intensities will be smaller, and so the spurious coincidence rate will also be smaller.

At the highest intensity (around $1.2 \times 10^6$ counts), the spurious coincidence rate can be calculated using the actual rate (coincidence of the two reference detectors), $\mathrm{R_{actual}}$, which is once again the average of all counts at that intensity, and the dark rate of the new monitor, $\mathrm{DR_{new}}$.

$$\mathrm{rate} = 2 \times w \times \mathrm{DR_{new}} \times \mathrm{R_{actual}} \tag{2}$$

This yields a spurious coincidence rate of 0.164 counts/s. This is around 7.099e-05 % of the actual hits measured, which can once again be considered negligible.

## VII. Conclusions

The full beam intensity monitor prototype has been assembled and tested. The required parts for the optical component gluing were designed and 3D printed, and the full assembly was put together. Preliminary tests were conducted using cosmics, and the grooved light guide was chosen due to its higher efficiency. Full tests were conducted in the beamline to give efficiencies that were mostly over 99.5%, which exceeds the target efficiency of 98%.

From these results, this design for the new intensity monitor looks promising. It is recommended that a round of mechanical changes be made based on the suggestions in Section VIII A, in addition to testing the detector under vacuum and verifying the functionality of the motorization. Additionally, tests at high intensity (larger than $10^7$ counts) are planned for 2026, to ensure that the monitor can operate at the full possible intensity range. After these are completed, this new design can be implemented to replace the existing XSCI intensity monitors.

## VIII. Appendix

### A. Mechanical Improvements

During the assembly and installation process, there were aspects of the mechanical assembly that could be modified to make the process easier. They will be listed here as a reference for future designs.

#### *1. Light Guide Tolerancing*

First, the main issue encountered in the gluing process was the fishtail light guide tolerancing. There are three main issues here:

- The groove was not the correct size for the flat light guides. This resulted in the machining and sanding/polishing already described, as well as difficulties getting the flat light guide into the groove without any air bubbles getting trapped during the gluing process.
- The circular end was too large for the clip. This meant that the vacuum test was not performed, as there was not adequate pressure holding the optical window and light guide in place.
- The additional machining on the groove meant that the groove ended up quite deep - this 'cut in' to the angular part of the light guide, so that the flat light guide ends up being slightly larger than the bottom of the groove. This is not a significant effect, but if similar light guides are ordered in the future, this could be taken into consideration.

#### *2. Assembly*

When attaching the ring clamp on the scintillator assembly to the optical window assembly, it was fairly difficult to put on the small nuts to hold the two together. This was mainly due to the narrow working area. A potential solution would be to widen the top part of the hole through the flange, which could make it easier to get the nuts in place. Additionally, the bolts coming out of the optical window assembly were a bit too close to the edge of the ring clamp/the light guide, adding to the difficulties of putting the nuts on.

*3. Flange holes*

This is a known issue, but the flange holes will need to be remachined to proceed with the vacuum test.

*4. PMT base sizes*

This may or may not be a huge concern in the future, but not all PMT bases were compatible with the optical window assembly. One PMT base had a very slightly smaller inner radius, such that it could not fit all the way on the assembly. The type/size of PMT base should be verified before large quantities are produced or ordered.

## IX. Acknowledgments

I would like to thank Inaki Ortega and Robert Larsen for their guidance and support on this project and for everything they have taught me. Thank you to Mark Kirschbaum for designing this project, as well as the rest of the SY-BI-XEI section for their help. I would also like to thank the Institute of Particle Physics (IPP), NSERC, and CERN for the financial support enabling my participation in the CERN summer student programme.

---

[1] CERN, "The Large Hadron Collider." Available: https://home.cern/science/accelerators/old-large-hadron-collider, 2025. Accessed: 18-08-2025.

[2] Beam Instrumentation (BI), "Beam instrumentation group." Available: https://sy-dep-bi.web.cern.ch/content/beam-instrumentation-group. Accessed: 18-08-2025.

[3] CERN Accelerators Department Beam Instrumentation Group, "System Portal: BXSCINT." Available: https://confluence.cern.ch/pages/viewpage.action?spaceKey=BEBI&title=System+portal+ Accessed: 18-08-2025.

[4] D. Banerjee, J. Bernhard, M. Brugger, N. Charitonidis, N. Doble, L. Gatignon, and A. Gerbershagen, "The North Experimental Area at the Cern Super Proton Synchrotron," 2021. Dedicated to Giorgio Brianti on the 50th anniversary of his founding the SPS Experimental Areas Group of CERN-Lab II and hence initiating the present Enterprise.

[5] M. Kirschbaum, "A New Beam Intensity Monitor for the CERN North Experimental Area," Master's thesis, Darmstadt University of Technology, 2024.

[6] H. Kolanoski and N. Wermes, *Particle Detectors: Fundamentals and Applications.* Oxford University Press, 06 2020.

[7] CERN Accelerators Department Beam Instrumentation Group, "System Portal: BXFISC." Available: https://confluence.cern.ch/display/BEBI/System+portal+ Accessed: 18-08-2025.

[8] W. Leo, *Techniques for Nuclear and Particle Physics Experiments: A How-To Approach.* Springer Berlin Heidelberg, 1994.

[9] V. Bocci, "A simple model for multiple coincidence sipm dark noise," 2024.